© 2014. Published by The Company of Biologists Ltd | Development (2014) 141, 2165-2171 doi:10.1242/dev.105072

RESEARCH ARTICLE

TECHNIQUES AND RESOURCES

Highly efficient targeted mutagenesis in axolotl using Cas9 RNA-guided nuclease

G. Parker Flowers[1], Andrew T. Timberlake[1], Kaitlin C. Mclean[1], James R. Monaghan[2] and Craig M. Crews[1,3,4,*]

ABSTRACT

Among tetrapods, only urodele salamanders, such as the axolotl *Ambystoma mexicanum*, can completely regenerate limbs as adults. The mystery of why salamanders, but not other animals, possess this ability has for generations captivated scientists seeking to induce this phenomenon in other vertebrates. Although many recent advances in molecular biology have allowed limb regeneration and tissue repair in the axolotl to be investigated in increasing detail, the molecular toolkit for the study of this process has been limited. Here, we report that the CRISPR-Cas9 RNA-guided nuclease system can efficiently create mutations at targeted sites within the axolotl genome. We identify individual animals treated with RNA-guided nucleases that have mutation frequencies close to 100% at targeted sites. We employ this technique to completely functionally ablate EGFP expression in transgenic animals and recapitulate developmental phenotypes produced by loss of the conserved gene *brachyury*. Thus, this advance allows a reverse genetic approach in the axolotl and will undoubtedly provide invaluable insight into the mechanisms of salamanders' unique regenerative ability.

KEY WORDS: Axolotl, CRISPR, Regeneration, Mutagenesis

INTRODUCTION

Historically, the axolotl, or *Ambystoma mexicanum*, has been a valuable organism to developmental biologists. Most significantly, the axolotl is capable of remarkable feats of adult regeneration including regeneration of the limbs, tail, brain, spinal chord, jaw and heart after injury (Lepperdinger et al., 2008). Given that urodele amphibians are the only vertebrates capable of completely regenerating limbs as adults, unraveling the mechanisms of this ideal form of vertebrate regeneration has long been a goal of regeneration biology. Using high-throughput sequencing and microarray analyses, several laboratories have recently generated lists of genes associated with the regeneration of particular tissues and structures in urodeles (Campbell et al., 2011; Holman et al., 2012; Knapp et al., 2013; Monaghan et al., 2009, 2012; Stewart et al., 2013; Wu et al., 2013); however, the identification of molecules and pathways implicated in regeneration has greatly outpaced the rate at which their function can be characterized in the animal.

The axolotl is a urodele widely used in regeneration studies as it is easily maintained and bred in the laboratory. Recently, several transgenic axolotl lines have been created to track cell fates and visualize the activation of signaling pathways during regeneration (Khattak et al., 2013a; Monaghan and Maden, 2012; Sobkow et al., 2006). The study of gene function in regeneration now benefits from several improvements in the delivery of exogenous DNA constructs into adult axolotl tissues (Khattak et al., 2013b; Whited et al., 2013); however, to date, no studies describe the targeted induction of mutations to perturb the function of endogenous genes. Such targeted loss-of-function mutations might enable the identification of genes that are essential for regeneration from the expanding lists of those specifically upregulated in regenerating tissues.

Several methods of inducing double-strand breaks in targeted sequences have been successfully employed to induce mutations in a variety of organisms and cell lines. Double-strand breaks are often imperfectly repaired by non-homologous end-joining (NHEJ) mechanisms that leave insertions or deletions (indels) at the break site. Methods of creating targeted indels include both synthetic targeted nucleases such as zinc-finger nucleases (ZFNs) and transactivator-like effector nucleases (TALENs), as well as RNA-guided nucleases (RGNs) such as the CRISPR-Cas9 system (Gaj et al., 2013). In the latter RGN system, a small guide RNA (sgRNA) complementary to a 20 base target DNA sequence guides an ectopically expressed, bacterially derived nuclease, Cas9, to induce a double-strand break at the target site (Hwang et al., 2013b). The relative ease of generating target-specific sgRNAs in the CRISPR-Cas9 RGN system, as compared with the more time-consuming assembly of novel chimeric nucleases with the TALEN and ZFN systems, makes RGNs particularly appealing. Although these methods are very promising, no work has yet described their efficacy in the axolotl.

Numerous studies demonstrate the efficacy of ZFNs, TALENs and RGNs at producing heritable mutations in organisms such as mouse, *C. elegans*, *Drosophila*, zebrafish and several plants (Gaj et al., 2013); however, a number of barriers impede the implementation of such technologies in the axolotl. The axolotl is not widely adopted as a genetic model organism due to its slow development, its late age of sexual maturity (>1 year), and its exceptionally large ($\sim 3.2\times10^{10}$ bp) and currently unsequenced genome (Smith et al., 2009). To overcome these drawbacks, the ideal practical system for investigating gene function in this organism must meet several seemingly daunting requirements. It must require little genomic sequencing information and must produce a very high rate of biallelic genome modifications to permit functional studies in F_o injected animals.

Here, we first demonstrate that RGNs can induce a very high rate of mutations in the *EGFP* locus of transgenic animals and consistently produce viable animals with little or no EGFP expression. We then show that this method can be used to produce mutations in a putative ortholog of an essential developmental gene, *brachyury*, recapitulating the loss-of-function phenotypes described in other organisms. We find that these phenotypes are associated with mutation rates approaching 100%. These results suggest that this system can reliably produce sufficiently high mutation rates such that a large percentage of injected animals

[1]Department of Molecular, Cellular, and Developmental Biology, Yale University, New Haven, CT 06511, USA. [2]Department of Biology, Northeastern University, Boston, MA 02115, USA. [3]Department of Chemistry, Yale University, New Haven, CT 06511, USA. [4]Department of Pharmacology, Yale University, New Haven, CT 06511, USA.

*Author for correspondence (craig.crews@yale.edu)

Received 18 October 2013; Accepted 17 March 2014

Development (2014) 141, 2165-2171 doi:10.1242/dev.105072

approximate true genetic knockouts. Our findings indicate that the CRISPR-Cas9 RGN system provides a robust method to investigate gene function in atypical model organisms.

RESULTS

RGN target selection and detection of indels in the axolotl

As the axolotl genome is currently unsequenced there are several challenges to the selection of RGN targets and assessment of mutation frequency that are not encountered in work with other organisms. Using stringent targeting constraints, so that the 20 base sgRNA targeting sequence must exactly match the intended DNA target, we only selected targets in which an NGG protospacer motif lies 18 bases downstream of a GG or GA sequence. These GG or GA bases at the 5′ end of the sgRNA correspond to the sequences incorporated by T7 or SP6 polymerases, respectively, following *in vitro* RNA syntheses. Such constraints allow the targeting of all sequences with the structure G(A/G)N_1…N_{19}GG to, on average, identify one target every ∼128 (or $1/4^3 \times 1/2$) bases of random sequence and, thus, once in every 64 bp of double-stranded DNA.

As the majority of publicly available axolotl genomic data comes from expressed sequence tag (EST) sequencing, and as the average intron length in the axolotl genome is greater than 10 kb (Smith et al., 2009), only a subset of targets found within EST sequences are spaced sufficiently far from intron-exon boundaries to be reliably detected with PCR-based methods. Rapid, endonuclease-based methods of screening pooled PCR products cannot be used to assess mutation frequency when putative mutation sites are near the edges of small PCR products. Thus, to initially assess the efficacy of this RGN system in the axolotl, we used a phenotypic, rather than genotypic, screening approach and selected targets that would produce unique, unambiguous phenotypes.

Functional ablation of *EGFP* in Tg(*CAGG:EGFP*) transgenic animals

We first tried to identify the optimal concentrations of sgRNA and *cas9* sufficient to induce observable loss of EGFP in the Tg(*CAGG:EGFP*) transgenic line (Sobkow et al., 2006). We injected various concentrations of *cas9* with an *EGFP*-directed sgRNA into embryos produced from a mating of a single-copy Tg(*CAGG:EGFP*) animal with a wild-type animal, ∼50% of which were expected to display uniform EGFP expression when not injected with RGNs. At several weeks post-injection, the viability of larvae injected with RGN was similar to those injected with mRNA encoding a neutral *nls-EGFP* (Fig. 1A). Although we observed little loss of *EGFP* in larvae injected with less than 100 pg sgRNA at any concentration of *cas9*, at the highest concentrations of *cas9* and sgRNA tested, namely 500 pg and 100 pg, respectively, we observed promising evidence of RGN activity (Fig. 1A). Observing animals under fluorescence, we found that, unlike their uninjected transgenic siblings which display uniform EGFP expression (Fig. 1B,C′), many RGN-injected animals displayed unambiguous loss of EGFP while retaining some EGFP expression (Fig. 1A,D,E′).

Of the surviving animals at 3 weeks post-injection, 87% were still viable 4 months post-injection (14 of 16), at which point all EGFP-negative animals were sacrificed. PCR of pooled DNA extracted from whole animals with no apparent EGFP expression revealed the presence of the Tg(*CAGG:EGFP*) transgene. Subsequent PCR analysis of DNA extracted from eight individual animals lacking EGFP expression revealed two apparently carrying the transgene, which suggests complete functional ablation of *EGFP*. We sequenced 32 clones from one such animal and found that they all contained indels at the targeted site (Fig. 1F). To determine whether the Tg(*CAGG:EGFP*) transgenic line contains a single integration or tandem integrations of the transgene, we carried out real-time quantitative PCR of *EGFP* from such animals. The results suggest that there is only single-copy integration of this transgene (supplementary material Fig. S1A).

Both our sequencing from an individual animal with no apparent EGFP expression and from two animals displaying very few EGFP-positive cells (supplementary material Fig. S1B) reveal numerous mutations per animal. Thus, in these cases, the high RGN-induced phenotype penetrance does not arise from mutations incurred within the first few cell divisions after development. Two subsequent injections of *cas9* with RGNs directed against *EGFP* produced embryos with non-Mendelian distributions of EGFP expression (3 of 23, and 4 of 13) at 2 weeks post-fertilization, and the remaining EGFP-positive embryos all displayed evident loss of EGFP. We have maintained several selected animals displaying extremely high levels of EGFP suppression for over 6 months (supplementary material Fig. S1C), indicating that high RGN-induced mutation rates can be achieved without long-term deleterious effects.

Efficient targeted mutagenesis of *brachyury* ortholog

After demonstrating the efficacy of RGNs at mutating single copies of *EGFP*, we then asked whether RGNs could produce phenotypes indicative of biallelic targeting. We directed RGNs against a presumptive ortholog of *brachyury*, which encodes a T-box transcription factor involved in cell-fate specification across phyla (Marcellini et al., 2003). In vertebrates, it is involved in mesoderm and, particularly, posterior somite specification (Martin and Kimelman, 2008).

At 3 weeks post-fertilization, we found that animals injected with *brachyury*-directed RGNs were significantly shorter along the anteroposterior axis than *nls-EGFP* mRNA-injected siblings [Fig. 2A,B; *brachyury* sgRNA injected, 1.9 cm (N=31); *nls-EGFP*, 2.3 cm (N=5); P=0.001, one-tailed Mann-Whitney U test]. At this stage, we classified the 15 out of 31 animals that were smaller than 1.9 cm, i.e. those more than four standard deviations shorter than non-RGN-injected controls, as displaying severe phenotypes (Fig. 2B; supplementary material Fig. S2). We extracted DNA from two whole truncated embryos and amplified, cloned, and sequenced the region flanking the targeted site. We found that this phenotype was associated with a high mutation rate, as 20 of 20 sequenced clones generated from one embryo and 17 of 18 from the other contained indels within the targeted sequence (Fig. 2D). We were able to maintain two severely truncated animals for more than 5 months post-injection (Fig. 2C). Ninety-three percent (26 of 26 clones from one animal and 17 of 20 from the other, i.e. 43 of 46) of sequenced PCR products from DNA extracted from fin clips in these animals contain indels at the expected site (Fig. 2E).

High rate of targeted mutagenesis at the *bambi* locus

We subsequently investigated whether we could efficiently mutate other genetic loci and identify highly mutant animals in the absence of a robust phenotype. We designed and injected an sgRNA against the BMP antagonist *bambi*, a gene highly expressed in limb blastemata (Knapp et al., 2013). We co-injected this sgRNA with *cas9* and *nls-EGFP* mRNAs. Despite injecting all animals at the one-cell stage, we found a surprising degree of variability in the distribution of NLS-EGFP expression after injection (supplementary material Fig. S3A,B). Whereas some embryos display uniform NLS-EGFP expression after injection, others display very localized or no NLS-EGFP expression, suggesting that injected mRNAs are often asymmetrically distributed or trapped in the yolk.

Development (2014) 141, 2165-2171 doi:10.1242/dev.105072

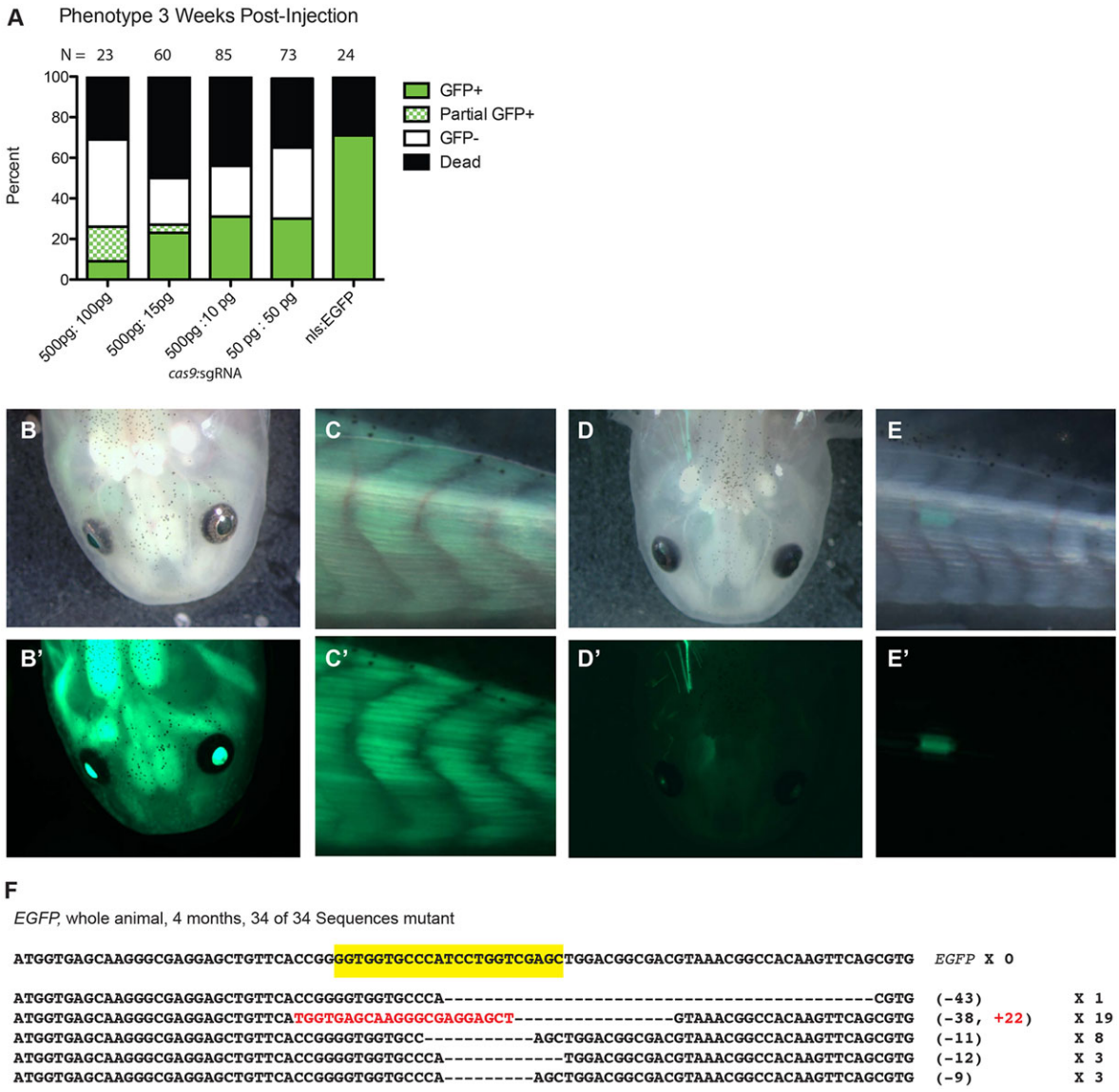

Fig. 1. Efficient targeted mutagenesis of *EGFP* in Tg(*CAGG:EGFP*) transgenic axolotls. (A) Distribution of phenotypes in axolotl (*Ambystoma mexicanum*) embryos from a mating between a wild-type and hemizygous Tg(*CAGG:EGFP*) animal injected with various concentrations of *cas9* mRNA and an *EGFP*-directed sgRNA at 3 weeks post-injection, as assessed by fluorescence microscopy. Whereas ~50% of embryos injected with lower concentrations of *cas9* and sgRNA displayed normal EGFP expression, those injected with the highest concentrations of *cas9* and sgRNA displayed mosaic EGFP expression. Any animal exhibiting clones of EGFP-negative cells was classified as 'partial EGFP'. The survival rate in all *cas9* and sgRNA-injected embryos did not differ from that of embryos injected with *nls-EGFP* mRNA only (right column). (B-E′) Whereas 6-month-old uninjected Tg(*CAGG:EGFP*) animals display strong uniform EGFP expression in both their heads (B′) and tails (C′), siblings injected with *EGFP*-directed sgRNA and *cas9* (D,E) display a dramatic loss of EGFP, with one individual with only EGFP-positive cells apparent in the head (D′) and another with EGFP expression only in the tail (E′). (B-E) Brightfield; (B′-E′) EGFP fluorescence. (F) All 34 sequences of cloned PCR products of the *EGFP* locus in a single animal injected with an *EGFP*-directed sgRNA and *cas9* that displayed no apparent EGFP expression contain indels at the targeted site (yellow). The size of each deletion (–) or insertion (+; in red) and frequency of occurrence among clones are indicated.

In the absence of a phenotype-based scoring system to identify probable mutant animals, we preselected uniformly EGFP-positive animals for further genotypic characterization. We first extracted DNA from three 1-week-old embryos displaying uniform NLS-EGFP expression and found that 25 of 33 clones sequenced from these animals displayed mutations within the targeted sequence (Fig. 3A). At several weeks post-injection we fin-clipped and extracted DNA from animals displaying similarly uniform NLS-EGFP expression, and found that 30 of 31 sequenced clones contained mutations at the targeted site, comprising 21 of 21, 6 of 7, and 3 of 3 in three animals (Fig. 3B). These fin-clipped, highly mutant animals are viable 5 months post-injection (Fig. 3C).

Together, our data suggest that this RGN system is highly applicable to the axolotl, as we have successfully produced viable animals bearing mutation rates greater than 90% at multiple targets.

DISCUSSION

The large genome, slow development and long generation time of the axolotl have hindered the use of the salamander as a model organism for studying the genetics of development, tissue repair and regeneration. Forward genetic screens to identify mutations

Development (2014) 141, 2165-2171 doi:10.1242/dev.105072

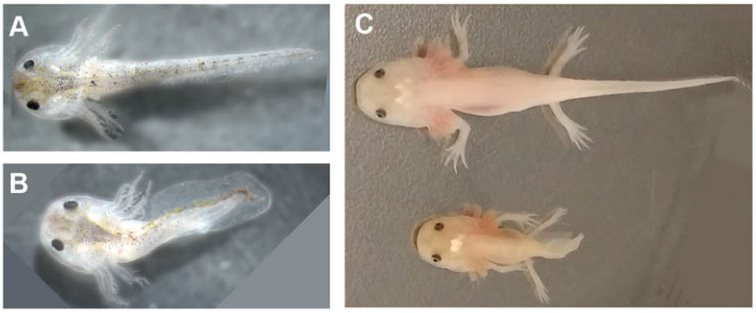

D *brachyury*, whole larva, day 21, 20 of 20 sequences mutant

```
ACGCTTACCCCCATAGCTGTTTCTCAGTCAGGAGGAATGCCTTCCGGTTTGGGGTCCCAGTAC WT        X 0
ACGCTTACCCCCATAGCTGTTTCTCAGTCAGGA------------------GGTCCCAGTAC (-19)
ACGCTTACCCCCATAGCTGTTTCTCAGTCAG---------------TTTGGGGTCCCAGTAC (-16)     X 6
ACGCTTACCCCCATAGCTGTTTCTCAGTCAGCCA------------GTTTGGGGTCCCAGTAC (-15, +3)
ACGCTTACCCCCATAGCTGTTTCTCAGTCAGGAGGAATGCCTT-------GGGGTCCCAGTAC (-7)
ACGCTTACCCCCATAGCTGTTTCTCAGTCAGGAGGAATGCCTT------TGGGGTCCCAGTAC (-6)
ACGCTTACCCCCATAGCTGTTTCTCAGTCAGGAGGAATGCCTTCCGG-----GGTCCCAGTAC (-5)      X 3
ACGCTTACCCCCATAGCTGTTTCTCAGTCAGGAGGAATGCCTTCCGG---GGGGTCCCAGTAC (-3)      X 7
```

brachyury, whole larva, day 21, 17 of 18 sequences mutant

```
ACGCTTACCCCCATAGCTGTTTCTCAGTCAGGAGGAATGCCTTCCGGTTTGGGGTCCCAGTAC WT        X 1
ACGCTTACCCCCATAGCTGTTTCT-------------------------TGGGGTCCCAGTAC (-25)     X 2
ACGCTTACCCCCATAGCTGTTTCTCAGTCAG--------------------GGTCCCAGTAC (-21)
ACGCTTACCCCCATAGCTGTTTCTCAGTCAGGAGG----------------GGTCCCAGTAC (-17)     X 2
ACGCTTACCCCCATAGCTGTTTCTCAGTCAGGAGGAATGCCTGGGGAATGA-GGTCCCAGTAC (-11, +10)X 3
ACGCTTACCCCCATAGCTGTTTCTCAGTCAGGAGGAATGCCTT------TGGGGTCCCAGTAC (-6)      X 4
ACGCTTACCCCCATAGCTGTTTCTCAGTCAGGAGGAATGCCTTCCGG-----GGTCCCAGTAC (-5)      X 5
```

E *brachyury*, fin clip, 5-months, 26 of 26 sequences mutant

```
ACGCTTACCCCCATAGCTGTTTCTCAGTCAGGAGGAATGCCTTCCGGTTTGGGGTCCCAGTAC WT        X 0
ACGCTTACCCCCATAGCTGTTTC----------------------------GGGTCCCAGTAC (-28)
ACGCTTACCCCCATAGCTGTTTCTCAGTCAGG--------------------GTCCCAGTAC (-21)     X 3
ACGCTTACCCCCATAGCTGTTTCTCAGTCAGGAG----------------GGGGTCCCAGTAC (-16)
ACGCTTACCCCCATAGCTGTTTCTCAGTCAGGAGGAATGCCT---------GGGTCCCAGTAC (-9)
ACGCTTACCCCCATAGCTGTTTCTCAGTCAGGAGGAATGCCTT-------GGGGTCCCAGTAC (-7)      X 2
ACGCTTACCCCCATAGCTGTTTCTCAGTCAGGAGGAATGCCTT------TGGGGTCCCAGTAC (-6)      X 11
ACGCTTACCCCCATAGCTGTTTCTCAGTCAGGAGGAATGCCTTCCGG-----GGTCCCAGTAC (-5)      X 3
ACGCTTACCCCCATAGCTGTTTCTCAGTCAGGAGGAATGCCTTCC--TTTGGGGTCCCAGTAC (-2)      X 4
```

brachyury, fin clip, 5-months,17 of 20 sequences mutant

```
ACGCTTACCCCCATAGCTGTTTCTCAGTCAGGAGGAATGCCTTCCGGTTTGGGGTCCCAGTAC WT        X 3
ACGCTTACCCCCATAGCTGTTTCTCAGTCAG--------------------GGTCCCAGTAC (-21)
ACGCTTACCCCCATAGCTGTTTCTCAGTCAGG-------------------GGTCCCAGTAC (-20)     X 2
ACGCTTACCCCCATAGCTGTTTCTCAGTCAG---------------TTTGGGGTCCCAGTAC (-16)
ACGCTTACCCCCATAGCTGTTTCTCAGTCAGGAGGA------------TTGGGGTCCCAGTAC (-12)
ACGCTTACCCCCATAGCTGTTTCTCAGTCAGGAGG------------TTTGGGGTCCCAGTAC (-12)
ACGCTTACCCCCATAGCTGTTTCTCAGTCAGGAGGAATGC------------GGTCCCAGTAC (-12)
ACGCTTACCCCCATAGCTGTTTCTCAGTCAGGAGGAATGCC----------GGGTCCCAGTAC (-10)     X 5
ACGCTTACCCCCATAGCTGTTTCTCAGTCAGGAGGAATGCC---------GGGGTCCCAGTAC (-9)
ACGCTTACCCCCATAGCTGTTTCTCAGTCAGGAGGAATGCCTT-------GGGGTCCCAGTAC (-7)
ACGCTTACCCCCATAGCTGTTTCTCAGTCAGGAGGAATGCCTTCCGG-----GGTCCCAGTAC (-5)
ACGCTTACCCCCATAGCTGTTTCTCAGTCAGGAGGAATGCCTTCC----TGGGGTCCCAGTAC (-4)
ACGCTTACCCCCATAGCTGTTTCTCAGTCAGGAGGAATGCCTTCCGGT----GGTCCCAGTAC (-4)
```

Fig. 2. Efficient targeted mutagenesis of *brachyury* ortholog. (A,B) Whereas animals injected with *nls-EGFP* mRNA display no phenotype at 21 days post-fertilization (A), their siblings injected with sgRNA directed against a putative *brachyury* ortholog and *cas9* display a dramatic shortening along the anteroposterior axis (B). (C) This phenotype persists at 7 months post-fertilization, as an sgRNA-injected animal (bottom) shows a severe reduction in length of the posterior body compared with an *nls-EGFP*-injected sibling (top). (D) Sequencing of the targeted region from two *brachyury* RGN-injected 21-day-old whole larvae displaying a severe phenotype as in B reveal a high indel frequency at the targeted site. (E) Sequencing of the targeted region from DNA extracted from fin clips of two *brachyury* RGN-injected 5-month-old animals displaying a severe phenotype as in C reveals a high indel frequency at this site.

affecting these processes cannot be carried out within a reasonable time frame, and reverse genetics using homologous recombination is particularly challenging in anamniotic vertebrates. Recent innovations in targeted mutagenesis using DNA-modifying enzymes have enabled the generation of frogs, fish and newts with mutations in targeted genes (Hwang et al., 2013a; Ishibashi et al., 2012; Lei et al., 2012; Hayashi et al., 2014), and here we provide the first demonstration of the successful application of such a technique in the axolotl. As a wealth of information about genes implicated in urodele limb regeneration has been compiled over decades of research using the axolotl, DNA-modifying enzymes and RGNs now make possible a reverse genetic approach for the characterization of these genes *in vivo*.

The large genome of urodeles provides potential challenges to the application of RGNs and other targeted DNA-modifying enzymes. The axolotl genome is approximately one order of magnitude larger than the next largest animal genome in which RGN-driven genetic modification has been described. The vast majority of the genome is unsequenced, and most of the available data come from EST sequencing. Using such data as a guide, RGN target selection is limited to targets that can be amplified with primers falling within the targeted exons as, at 10 kb, the average distance between exons in the axolotl genome is too large to reliably amplify across. To permit the identification of most RGN-induced indels, targets must be at least one primer length away from intron-exon boundaries. In this study, The *bambi* ortholog was amplified with a primer 13 bases

Development (2014) 141, 2165-2171 doi:10.1242/dev.105072

A

bambi, 3 whole embryos, day 5, 25 of 33 mutant

```
ACCTCTGTCGGGCGAGGAAGGCCCCCAACCACACGGGCACCGCCACCCCCAGGCTGGAGTGCTGCCACGAAGACATGTGC   WT     X 8
ACCTCTGTCGGGCGAGGAAGGCCCC----------------GCCACCCCCAGGCTGGAGTGCTGCCACGAAGACATGTGC  (-16)
ACCTCTGTCGGGCGAGGAAGGCCCCCAGC---ACGGGCACCGCCACCCCCAGGCTGGAGTGCTGCCACGAAGACATGTGC  (-4, +1)
ACCTCTGTCGGGCGAGGAAGGCCCCCAAC---ATGGGCACCGCCACCCCCAGGCTGGAGTGCTGCCACGAAGACATGTGC  (-4, +1)
ACCTCTGTCGGGCGAGGAAGGCC----ACCACACGGGCACCGCCACCCCCAGGCTGGAGTGCTGCCACGAAGACATGTGC  (-4)
ACCTCTGTCGGGCGAGGAAGGCCCCCAACCA----GGCACCGCCACCCCCAGGCTGGAGTGCTGCCACGAAGACATGTGC  (-4)
ACCTCTGTCGGGCGAGGAAGGCCCCCAAC---ACGGGCACCGCCACCCCCAGGCTGGAGTGCTGCCACGAAGACATGTGC  (-3)    X 20
```

B

bambi, fin clip, 1 month, A, 21 of 21 mutant

```
ACCTCTGTCGGGCGAGGAAGGCCCCCAACCACACGGGCACCGCCACCCCCAGGCTGGAGTGCTGCCACGAAGACATGTGC  WT     X 0
ACCTCTGTCGG----------------------------------ACCCCCAGGCTGGAGTGCTGCCACGAAGACATGTGC  (-33)
ACCTCTGTCGGGCGAGGAAGG--------------------------------TGGAGTGCTGCCACGAAGACATGTGC  (-33)  X 2
ACCTCTGTCGGGCGAGGAAGG-----------------------------GGCTGGAGTGCTGCCACGAAGACATGTGC  (-30)  X 2
ACCTCTGTCGGGCGAGGAAGGCC--------------CACCGCCACCCCCAGGCTGGAGTGCTGCCACGAAGACATGTGC  (-14)  X 2
ACCTCTGTCGGGCGAGGAAGGCC----ACCACACGGGCACCGCCACCCCCAGGCTGGAGTGCTGCCACGAAGACATGTGC  (-4)   X 4
ACCTCTGTCGGGCGAGGAAGGCCCCCAAC---ACGGGCACCGCCACCCCCAGGCTGGAGTGCTGCCACGAAGACATGTGC  (-3)   X 10
```

bambi, fin clip, 1 month, B, 6 of 7 mutant

```
ACCTCTGTCGGGCGAGGAAGGCCCCCAACCACACGGGCACCGCCACCCCCAGGCTGGAGTGCTGCCACGAAGACATGTGC  WT     X 1
ACCTCTGTCGGGCGAGGAAGGCC------------------GCCACCCCCAGGCTGGAGTGCTGCCACGAAGACATGTGC  (-18)
ACCTCTGTCGGGCGAGGAAGGCCCCCAAC---ACGGGCACCGCCACCCCCAGGCTGGAGTGCTGCCACGAAGACATGTGC  (-3)   X 5
```

bambi, fin clip, 1 month, C, 3 of 3 mutant

```
ACCTCTGTCGGGCGAGGAAGGCCCCCAACCACACGGGCACCGCCACCCCCAGGCTGGAGTGCTGCCACGAAGACATGTGC  WT     X 0
ACCTCTGTCGGGCGAGGAAGGCCCCCAAC---ACGGGCACCGCCACCCCCAGGCTGGAGTGCTGCCACGAAGACATGTGC  (-3) X 3
```

C

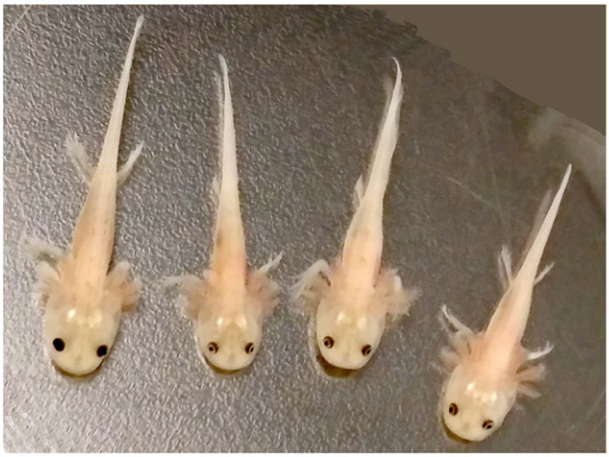

Fig. 3. Efficient targeted mutagenesis at the *bambi* locus. (A) Sequencing of the targeted region of the *bambi* locus from three *bambi* RGN-injected 5-day-old whole embryos reveals a high indel frequency at the targeted site. (B) Sequencing of the targeted region of the *bambi* locus from DNA extracted from fin clips of three *bambi* RGN-injected 1-month-old embryos reveals a high indel frequency at the targeted site. (C) A sibling control (left) and the three *bambi* mutant embryos with the reported (see B) A, B and C genotypes (left to right, respectively), at 4 months.

away from the targeted sequence, while the *brachyury* ortholog was successfully amplified with a primer only two bases away from the targeted sequence. Although the majority of RGN-induced indels described here and elsewhere in larger PCR amplicons do not extend beyond two bases outside of the targeted sequence, RGNs can produce much larger indels. As indels that eliminate the targets of the primers used for genotyping are undetectable, the already very high mutation rates that we report in animals in which we targeted *bambi* and *brachyury* are likely to underestimate the true mutation frequencies. Thus, while the target selection criteria used in this study identify, on average, one target in every 64 bases of random sequence, incomplete genomic information places additional constraints on target selection. These challenges to RGN design and efficacy assessment will undoubtedly be ameliorated by efforts to sequence the axolotl genome that are currently underway.

Although our initial experiments with *EGFP* and a *brachyury* ortholog suggest that individual animals with mutation frequencies of, or very close to, 100% can be produced using this method, we often observed animals without apparent phenotypes. Such variability can pose challenges to the analysis of RGN-injected animals. While stochastic qualities of RGN activity and NHEJ repair may contribute to this variability, we expect that much of this variation arises from the injections. We find that when we co-inject an *nls-EGFP* mRNA tracer with RGNs into one-cell embryos, the distribution of this tracer is non-uniform in the developing embryos. As the axolotl embryo is particularly rich in yolk, this might impede the diffusion of injected materials. When we preselect embryos displaying widespread *EGFP* expression, we find that the mutation rates in such embryos are similar to those that have been preselected by phenotype (i.e. animals lacking EGFP or displaying the *brachyury* phenotype). Thus, similar methods of prescreening embryos after RGN injection might greatly facilitate the process of identifying highly mutant animals.

Recent work demonstrates that complete homology of the 5′ end of the sgRNA to the targeted DNA sequence is not required for efficient indel induction; thus, the targeting constraints may be loosened to allow the targeting of every 18 base sequence preceding

Development (2014) 141, 2165-2171 doi:10.1242/dev.105072

an NGG (~1 in every 8 bases) (Hwang et al., 2013a). Although such loosened constraints could permit the identification of numerous targets in each gene of interest using only fragmentary EST data, in this study we did not attempt to target genes with these relaxed criteria. Additional work demonstrated that in cell lines transfected with Cas9-encoding plasmids and various sgRNAs, indels were sometimes observed with high frequency in sites with as many as five mismatches from the guide sequence (Fu et al., 2013). Presumably, off-target activity might be similarly high in axolotls injected with RGNs, but we have limited means or reference to assess this by sequencing. We have seen surprisingly little evidence of gross toxicity or teratogenicity of RGNs at concentrations sufficient to highly mutate developmentally neutral genes such as *EGFP*, and animals in which *brachyury* is highly mutated are viable despite the profound phenotype. As RGNs show great promise as a means of probing the function of novel genes with uncharacterized phenotypes, great care must be taken to confirm that phenotypes in RGN-treated animals are associated with loss of function of the targeted gene. Although off-target mutations can be selected against by outcrossing mutant lines for several generations, the time frame required by this approach is not practical for experiments with an organism with a long generation time. Thus, phenotypes should be confirmed in mutants created with sgRNAs directed against different targets within the same gene, and, when possible, rescue experiments should be conducted using recent innovations in exogenous gene delivery and inducible gene expression in the axolotl (Khattak et al., 2013b; Whited et al., 2012, 2013).

Our studies demonstrate that RGNs can be effectively used to produce viable individual axolotls with mutation rates nearing 100% at targeted sites. This technique will be invaluable in investigating the molecular bases of the remarkable regenerative capability of the axolotl. Furthermore, the high frequency of mutagenesis and corresponding phenotypes in injected embryos suggest that the axolotl is an accessible organism for comparative developmental genetic studies. Despite the challenges posed by the size of the axolotl genome, we achieved high rates of targeted mutagenesis using only partial EST sequencing data. Current efforts to sequence the axolotl genome will greatly facilitate subsequent analysis of gene function using this system. These results suggest that this RGN system of targeted mutagenesis might provide a powerful means to carry out reverse genetic studies in other less traditional model organisms using limited genomic information.

MATERIALS AND METHODS

Target identification

The EST sequences corresponding to an axolotl *brachyury* ortholog were identified on Sal-Site (http://www.ambystoma.org) (Smith et al., 2005) and correspond to contig C2459046 in assembly 4. The *bambi* ortholog corresponds to the sequence of *dk17* on Axolotl (http://est.age.mpg.de/in-situ/html_20111118/DK17.html) as described by Knapp et al. (2013).

Plasmids and RNA synthesis

We transcribed *cas9* mRNA from the *MLM3613* vector using T7 mMessage mMachine and PolyA tailing kits (Life Technologies) as described (Hwang et al., 2013b). sgRNA templates were made using *Dr274* as previously described (Hwang et al., 2013b). For each target we annealed the following oligonucleotide pairs and ligated this product into *Bsa*I-linearized *Dr274*: to generate an sgRNA to target 5′-GGTGCCCATCCTGGTCGAGC-3′ of the Tg(*CAGG:EGFP*) transgene, 5′-TAGGTGCCCATCCTGGTCGAGC-3′ and 5′-AACGCTCGACCAGGATGGGCA; to target the 5′-GGAGGAATGCCT-TCCGGTTT-3′ of *brachyury*, 5′-TAGGAGGAATGCCTTCCGGTTT-3′ and 5′-AACCAAACCGGAAGGCATTCCT-3′; and to target 5′-GGCGGTGCCC-GTGTGGTTGG-3′ of *bambi*, 5′-TAGGCGGTGCCCGTGTGGTTGG-3′ and 5′-AAACCCAACCACACGGGCACCG-3′. These templates were linearized with *Dra*I, and sgRNAs were transcribed from this template with the T7 Maxiscript kit (Life Technologies). After DNase digestion of templates, mRNA and sgRNA were purified by phenol:choloroform extraction and ammonium acetate precipitation before resuspension in RNase-free water.

Embryo microinjection

All embryos were generated from natural matings. Embryos were manually dejellied in 1× MMR and transferred to 1× MMR with 20% Ficoll (Sigma-Aldrich) as described (Khattak et al., 2009). Embryos were microinjected with mRNA and sgRNA in 3 nl droplets. Injections of sgRNA targeting EGFP were at the concentrations described in Fig. 1A, whereas all subsequent injections used 3 nl droplets containing 500 pg *cas9* mRNA, 100 pg sgRNA and 50 pg *nls-EGFP* mRNA. After several hours, injected embryos were transferred to 0.1× MMR in 5% Ficoll. After 24 h, we transferred embryos to 0.1× MMR and maintained them as described (Khattak et al., 2009). For several weeks post-injection, embryos were monitored daily under a stereomicroscope, and any unfertilized embryos or embryos leaking yolk were removed.

DNA extraction

EGFP-negative animals from the group of animals injected with 500 pg *cas9* mRNA and 100 pg sgRNA described in Fig. 1A were euthanized at 4 months post-injection in 3 mg/ml Tricaine (Sigma-Aldrich). DNA was extracted from whole animals using the DNeasy Blood and Tissue Kit (Qiagen). DNA was similarly extracted from several embryos injected with *brachyury* sgRNA and *cas9* mRNA as shown in Fig. 2B. DNA was extracted from fin clips of two 5-month-old embryos displaying the phenotype depicted in Fig. 2C. We extracted pooled DNA from three whole embryos injected with *bambi*-directed sgRNA, *cas9* and *nls-EGFP* mRNAs displaying uniform nls-EGFP expression at 5 days post-injection. We found that nls-EGFP expression was still evident at 4 weeks post-injection, at which point we extracted DNA from fin clips of three nls-EGFP-positive animals.

PCR and cloning

The following primers (5′-3′) were used for cloning the described targets: *EGFP* forward, GCAACGTGCTGGTTATTGTG; *EGFP* reverse, AAGTC-GTGCTGCTTCATGTG; *brachyury* forward, CCCAATTTGTGGTCTGTG; *brachyury* reverse, CGTAAGTACTGGGACCC; *bambi* forward, GACCCC-CAGAACTCCAACTC; *bambi* reverse, ATGTCTTCGTGGCAGCACTC-3′. PCR products were cloned with the pGEM-T Easy vector system (Promega) and positive colonies were sequenced.

Real-time quantitative PCR

All PCRs were performed on a Bio-Rad CFX96 real-time system using IQ SYBR Green Supermix (Bio-Rad). Two sets of primers were used for the amplification of two distinct regions of the *EGFP* transgene producing 189 bp and 150 bp amplicons; two control sets of primers had melting temperatures that matched those of these primers. Primer sequences (5′-3′) are: EGFP189F, CCTGAAGTTCATCTGCACCA; EGFP189R, CCTGAAGTTCATCTGC-ACCA; EGFP150F, ACAAGCAGAAGAACGGCATC; EGFP150R, AC-TGGGTGCTCAGGTAGTGG; FGF189F, GGCACTACAAACGCCAAT; FGF189R, CTCCGCCTGTTGAAAGGATA; BAC150F, GTGGGGC-CATGTCTTAAGTG; BAC150R, GTGTACTCGGGGTTGTCGAT. Gel electrophoresis and melting curve analysis confirmed that all primer pairs produced a single, appropriately sized PCR product under the conditions employed. The EGFP189 and FGF189 primer pairs amplified under the following conditions: 60 s at 95°C, followed by 45 cycles of 95°C for 15 s and 60°C for 30 s. The EGFP150 and BAC150 primer pairs amplified under the following conditions: 95°C for 60 s, followed by 45 cycles of 15 s at 95°C and 30 s at 69°C. A series of three iterative 10-fold dilutions of genomic DNA extracted from a non-injected Tg(*CAGG:EGFP*) animal produced by the mating described in Fig. 1 was used as template for PCR. Each reaction was performed in duplicate and averaged numbers were used to create a standard curve. Reaction efficiencies and ΔCt scores were calculated as described (Bubner and Baldwin, 2004; Ginzinger, 2002).

Development (2014) 141, 2165-2171 doi:10.1242/dev.105072

Microscopy

Embryos were monitored and imaged with a Zeiss stereomicroscope using brightfield and GFP fluorescence. Animals over 1 month of age were anesthetized in 0.5 mg/ml Tricaine prior to imaging.

Acknowledgements

We thank Anne Jecrois for help with animal husbandry as well as Lennart Fiedler and Joseph Cusano for assistance with experiments.

Competing interests

The authors declare no competing interests.

Author contributions

G.P.F., J.R.M. and C.M.C. designed all experiments. G.P.F., A.T.T. and K.C.M. performed all experiments. G.P.F. wrote the manuscript. C.M.C. and J.R.M. edited the manuscript.

Funding

C.M.C. acknowledges the generous support of the Ellison Medical Foundation and the National Institutes of Health [R01GM094944]. A.T.T. was supported by a National Institutes of Health Medical Scientist Training Program Training Grant [T32GM007205]. Deposited in PMC for release after 12 months.

Supplementary material

Supplementary material available online at
http://dev.biologists.org/lookup/suppl/doi:10.1242/dev.105072/-/DC1

References

Bubner, B. and Baldwin, I. T. (2004). Use of real-time PCR for determining copy number and zygosity in transgenic plants. *Plant Cell Rep.* **23**, 263-271.

Campbell, L. J., Suárez-Castillo, E. C., Ortiz-Zuazaga, H., Knapp, D., Tanaka, E. M. and Crews, C. M. (2011). Gene expression profile of the regeneration epithelium during axolotl limb regeneration. *Dev. Dyn.* **240**, 1826-1840.

Fu, Y., Foden, J. A., Khayter, C., Maeder, M. L., Reyon, D., Joung, J. K. and Sander, J. D. (2013). High-frequency off-target mutagenesis induced by CRISPR-Cas nucleases in human cells. *Nat. Biotechnol.* **31**, 822-826.

Gaj, T., Gersbach, C. A. and Barbas, C. F. (2013). ZFN, TALEN, and CRISPR/Cas-based methods for genome engineering. *Trends Biotechnol.* **31**, 397-405.

Ginzinger, D. G. (2002). Gene quantification using real-time quantitative PCR. *Exp. Hematol.* **30**, 503-512.

Hayashi, T., Sakamoto, K., Sakuma, T., Yokotani, N., Inoue, T., Kawaguchi, E., Agata, K., Yamamoto, T. and Takeuchi, T. (2014). Transcription activator-like effector nucleases efficiently disrupt the target gene in Iberian ribbed newts (Pleurodeles waltl), an experimental model animal for regeneration. *Dev. Growth Differ.* **56**, 115-121.

Holman, E. C., Campbell, L. J., Hines, J. and Crews, C. M. (2012). Microarray analysis of microRNA expression during axolotl limb regeneration. *PLoS ONE* **7**, e41804.

Hwang, W. Y., Fu, Y., Reyon, D., Maeder, M. L., Kaini, P., Sander, J. D., Joung, J. K., Peterson, R. T. and Yeh, J.-R. J. (2013a). Heritable and precise zebrafish genome editing using a CRISPR-Cas system. *PLoS ONE* **8**, e68708.

Hwang, W. Y., Fu, Y., Reyon, D., Maeder, M. L., Tsai, S. Q., Sander, J. D., Peterson, R. T., Yeh, J.-R. J. and Joung, J. K. (2013b). Efficient genome editing in zebrafish using a CRISPR-Cas system. *Nat. Biotechnol.* **31**, 227-229.

Ishibashi, S., Cliffe, R. and Amaya, E. (2012). Highly efficient bi-allelic mutation rates using TALENs in Xenopus tropicalis. *Biol. Open* **1**, 1273-1276.

Khattak, S., Richter, T. and Tanaka, E. M. (2009). Generation of transgenic axolotls (Ambystoma mexicanum). *Cold Spring Harb. Protoc.* **2009**, db.prot5264.

Khattak, S., Schuez, M., Richter, T., Knapp, D., Haigo, S. L., Sandoval-Guzmán, T., Hradlikova, K., Duemmler, A., Kerney, R. and Tanaka, E. M. (2013a). Germline transgenic methods for tracking cells and testing gene function during regeneration in the axolotl. *Stem Cell Rep.* **1**, 90-103.

Khattak, S., Sandoval-Guzmán, T., Stanke, N., Protze, S., Tanaka, E. M. and Lindemann, D. (2013b). Foamy virus for efficient gene transfer in regeneration studies. *BMC Dev. Biol.* **13**, 17.

Knapp, D., Schulz, H., Rascon, C. A., Volkmer, M., Scholz, J., Nacu, E., Le, M., Novozhilov, S., Tazaki, A., Protze, S. et al. (2013). Comparative transcriptional profiling of the axolotl limb identifies a tripartite regeneration-specific gene program. *PLoS ONE* **8**, e61352.

Lei, Y., Guo, X., Liu, Y., Cao, Y., Deng, Y., Chen, X., Cheng, C. H. K., Dawid, I. B., Chen, Y. and Zhao, H. (2012). Efficient targeted gene disruption in Xenopus embryos using engineered transcription activator-like effector nucleases (TALENs). *Proc. Natl. Acad. Sci. U.S.A.* **109**, 17484-17489.

Lepperdinger, G., Roy, S. and Gatien, S. (2008). Regeneration in axolotls: a model to aim for! *Exp. Gerontol.* **43**, 968-973.

Marcellini, S., Technau, U., Smith, J. C. and Lemaire, P. (2003). Evolution of Brachyury proteins: identification of a novel regulatory domain conserved within Bilateria. *Dev. Biol.* **260**, 352-361.

Martin, B. L. and Kimelman, D. (2008). Regulation of canonical Wnt signaling by brachyury is essential for posterior mesoderm formation. *Dev. Cell* **15**, 121-133.

Monaghan, J. R. and Maden, M. (2012). Visualization of retinoic acid signaling in transgenic axolotls during limb development and regeneration. *Dev. Biol.* **368**, 63-75.

Monaghan, J. R., Epp, L. G., Putta, S., Page, R. B., Walker, J. A., Beachy, C. K., Zhu, W., Pao, G. M., Verma, I. M., Hunter, T. et al. (2009). Microarray and cDNA sequence analysis of transcription during nerve-dependent limb regeneration. *BMC Biol.* **7**, 1.

Monaghan, J. R., Athippozhy, A., Seifert, A. W., Putta, S., Stromberg, A. J., Maden, M., Gardiner, D. M. and Voss, S. R. (2012). Gene expression patterns specific to the regenerating limb of the Mexican axolotl. *Biol. Open* **1**, 937-948.

Smith, J. J., Putta, S., Walker, J. A., Kump, D. K., Samuels, A. K., Monaghan, J. R., Weisrock, D. W., Staben, C. and Voss, S. R. (2005). Sal-site: integrating new and existing ambystomatid salamander research and informational resources. *BMC Genomics* **6**, 181.

Smith, J. J., Putta, S., Zhu, W., Pao, G. M., Verma, I. M., Hunter, T., Bryant, S. V., Gardiner, D. M., Harkins, T. T. and Voss, S. R. (2009). Genic regions of a large salamander genome contain long introns and novel genes. *BMC Genomics* **10**, 19.

Sobkow, L., Epperlein, H.-H., Herklotz, S., Straube, W. L. and Tanaka, E. M. (2006). A germline GFP transgenic axolotl and its use to track cell fate: dual origin of the fin mesenchyme during development and the fate of blood cells during regeneration. *Dev. Biol.* **290**, 386-397.

Stewart, R., Rascón, C. A., Tian, S., Nie, J., Barry, C., Chu, L.-F., Ardalani, H., Wagner, R. J., Probasco, M. D., Bolin, J. M. et al. (2013). Comparative RNA-seq analysis in the unsequenced axolotl: the oncogene burst highlights early gene expression in the blastema. *PLoS Comput. Biol.* **9**, e1002936.

Whited, J. L., Lehoczky, J. A. and Tabin, C. J. (2012). Inducible genetic system for the axolotl. *Proc. Natl. Acad. Sci. U.S.A.* **109**, 13662-13667.

Whited, J. L., Tsai, S. L., Beier, K. T., White, J. N., Piekarski, N., Hanken, J., Cepko, C. L. and Tabin, C. J. (2013). Pseudotyped retroviruses for infecting axolotl in vivo and in vitro. *Development* **140**, 1137-1146.

Wu, C.-H., Tsai, M.-H., Ho, C.-C., Chen, C.-Y. and Lee, H.-S. (2013). De novo transcriptome sequencing of axolotl blastema for identification of differentially expressed genes during limb regeneration. *BMC Genomics* **14**, 434.